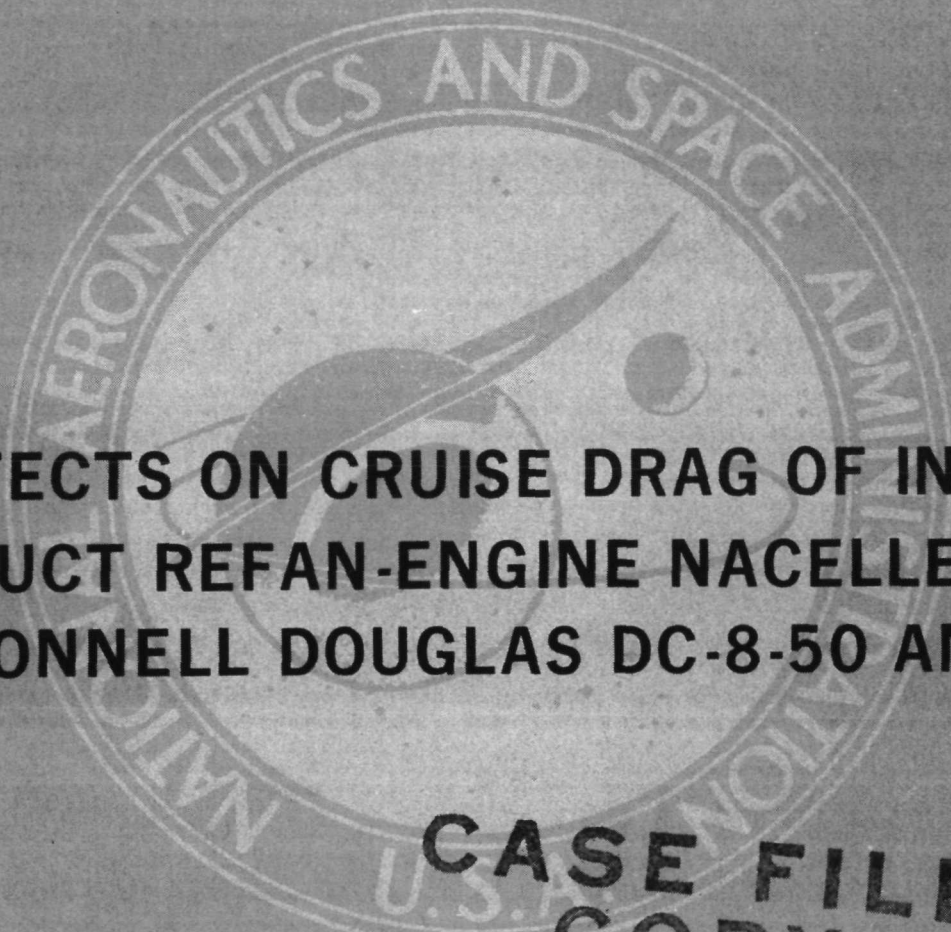


N 7 3 2 6 0 2 3

NASA CR-121218  
REPORT MDC J5947



# THE EFFECTS ON CRUISE DRAG OF INSTALLING LONG-DUCT REFAN-ENGINE NACELLES ON THE MCDONNELL DOUGLAS DC-8-50 AND -61

**CASE FILE  
COPY**

by J. T. CALLAGHAN, J. E. DONELSON AND J. P. MORELLI

prepared for  
NATIONAL AERONAUTICS AND SPACE ADMINISTRATION  
NASA Lewis Research Center  
Contract NAS 3-16814

**DOUGLAS AIRCRAFT COMPANY**

**MCDONNELL DOUGLAS**





1. Report No. NASA CR-121218		2. Government Accession No.		3. Recipient's Catalog No.	
4. Title and Subtitle The Effects on Cruise Drag of Installing Long-Duct Refan-Engine Nacelles on the McDonnell-Douglas DC-8-50 and -61				5. Report Date May 1973	
				6. Performing Organization Code	
7. Author(s) J. T. Callaghan, J. E. Donelson, and J. P. Morelli				8. Performing Organization Report No. MDC J5947	
9. Performing Organization Name and Address Douglas Aircraft Company Long Beach, California				10. Work Unit No.	
				11. Contract or Grant No. NAS 3-16814	
12. Sponsoring Agency Name and Address National Aeronautics and Space Administration Washington, D. C. 20546				13. Type of Report and Period Covered Contractor Report	
				14. Sponsoring Agency Code	
15. Supplementary Notes Project Manager, Arthur Medieros Research Center, Cleveland, Ohio NASA/Lewis					
16. Abstract  A high-speed wind tunnel test was conducted in the NASA Ames 11-foot facility in January 1973 to determine the effect on cruise performance of installing long-duct refan-engine nacelles on the DC-8-50 and -61 models. Drag data and wing/pylon/nacelle channel pressure data are presented. At a typical cruise condition there exists a very small interference drag penalty of less than one-percent of total cruise data for the Refan installation. Pressure data indicates that some supersonic flow is present in the inboard channel of the inboard refan nacelle installation, but it not sufficient to cause any wave drag on boundary layer separation. One pylon modification, which takes the form of pylon bumps, was tested. It resulted in a drag penalty, because its design goal of eliminating shock-related interference drag was not required and the bump thus became a source of additional parasite drag.					
17. Key Words (Suggested by Author(s))  DC-8 refanned long duct nacelle high speed pylon modifications			18. Distribution Statement		
19. Security Classif. (of this report) Unclassified		20. Security Classif. (of this page) Unclassified		21. No. of Pages 38	
				22. Price*	

\* For sale by the National Technical Information Service, Springfield, Virginia 22151



THE EFFECTS ON CRUISE DRAG OF  
INSTALLING LONG-DUCT REFAN-ENGINE NACELLES  
ON THE MCDONNELL-DOUGLAS DC-8-50 AND -61

by J. T. Callaghan, J. E. Donelson, and J. P. Morelli

MCDONNELL DOUGLAS CORPORATION

prepared for

NATIONAL AERONAUTICS AND SPACE ADMINISTRATION

NASA Lewis Research Center

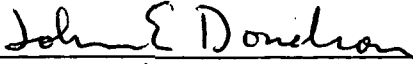
Contract NAS 3-16814



## FOREWORD

The high-speed wind tunnel test described in this report was performed by the Douglas Aircraft Company, Configuration Design Branch - Aerodynamics of the McDonnell Douglas Corporation. The work, sponsored by NASA Lewis and reported herein, was performed between January and April 1973.

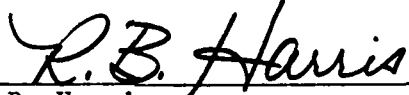
This report has been reviewed and is approved by:

  
J. E. Donelson  
NASA Refan Project Aerodynamicist


Date 5-14-73

  
F. T. Lynch, Chief  
Configuration Design Branch  
Aerodynamics

Date 5-14-73

  
R. B. Harris  
Chief Aerodynamics  
Engineer for Design

Date 5-17-73

  
O. R. Dunn  
Director of Aerodynamics

Date 5-17-73



## TABLE OF CONTENTS

	<u>Page</u>
1.0 SUMMARY . . . . .	1
2.0 INTRODUCTION . . . . .	3
3.0 SYMBOLS . . . . .	5
4.0 APPARATUS AND TEST . . . . .	7
4.1 Model Description . . . . .	7
4.1.1 Basic Model . . . . .	7
4.1.2 Nacelle Geometry . . . . .	7
4.1.3 Nacelle Installation Comparison . . . . .	8
4.1.4 Pylon Modifications . . . . .	8
4.2 Test Apparatus . . . . .	8
4.2.1 Facility and Model Installation . . . . .	8
4.2.2 Instrumentation . . . . .	9
4.3 Test Procedure and Data Accuracy . . . . .	9
5.0 RESULTS AND DISCUSSION . . . . .	11
5.1 Basic Refan Installation . . . . .	11
5.2 Pylon Modification . . . . .	12
6.0 CONCLUSIONS . . . . .	13
7.0 REFERENCES . . . . .	15
8.0 FIGURES . . . . .	17



## 1.0 SUMMARY

A high-speed wind tunnel test was conducted in the NASA Ames 11-foot facility in support of the NASA refan program in order to assess the effect on cruise performance of installing long-duct refan-engine nacelles on the DC-8-50 and -61 models, which currently have short-duct nacelle installations. This test was prompted by the desire to determine the feasibility of using a common long-duct refan-engine nacelle for all DC-8 models. Since the existing long-duct nacelles on the DC-8-62 and -63 models are farther forward of the wing leading edge than the short-duct nacelles, the refan installation was not considered to be a problem on those aircraft. The long-duct refan nacelle installed in the existing aft short-duct position of the Series 50 and 61, however, represented a potential interference drag problem due to the position of the nacelle relative to the wing. The purpose of this test was, therefore, to determine if an interference drag penalty existed for the installation of the long-duct refan nacelle on the existing Series 50 and 61 short-duct pylon, and, if necessary, to investigate potential fixes designed to minimize or eliminate the interference penalty. The potential fixes took the form of pylon bumps, which were designed to improve the area distribution in the channel formed by the wing, pylon, and nacelle.

Analysis of the results from this test leads to the following conclusions:

1. At a typical cruise condition there exists an interference drag penalty of less than one-percent of total cruise drag for the installation of the long-duct refan nacelle on the existing (minimum structural change) Series 50 and 61 short-duct pylon. This very small penalty would, however, be much more than off-set by the large improvement, demonstrated on the existing DC-8, of a long-duct nacelle over a short-duct nacelle.
2. At cruise conditions some supersonic flow is present in the inboard channel of the inboard refan-nacelle installation, but it is not sufficient to cause any wave drag or boundary layer separation. The small interference drag penalty results from a general thickening in the boundary layer of some of the components when they are integrated.

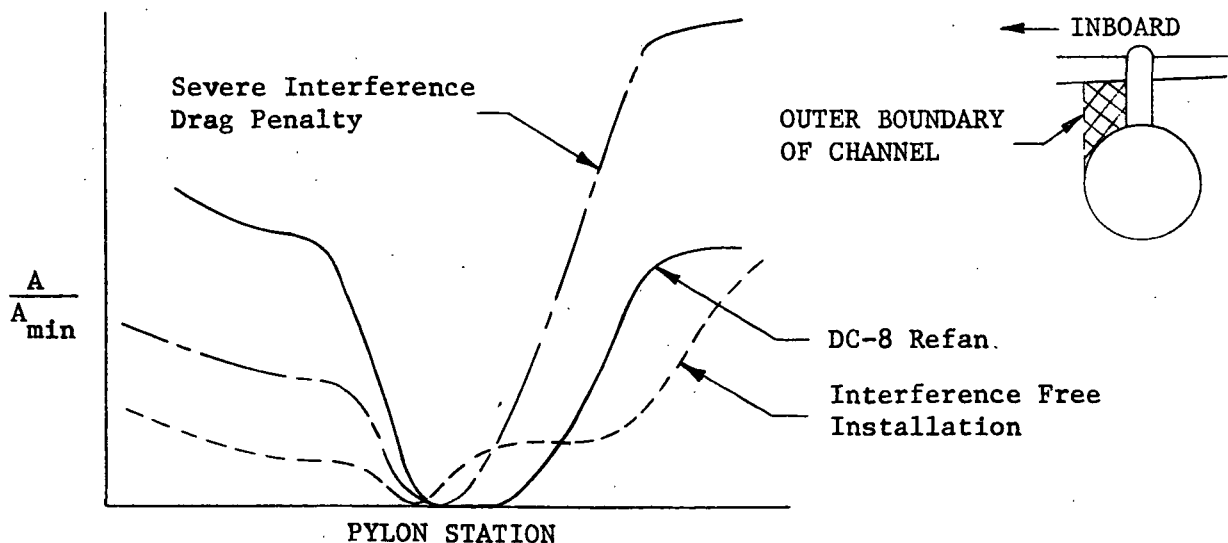


3. The one pylon modification tested resulted in a drag penalty, because its design goal of eliminating shock-related interference drag was not required and the bump thus became a source of additional parasite drag.
4. From aircraft performance considerations, a common long-duct refan-engine nacelle is certainly feasible for all DC-8 models.



## 2.0 INTRODUCTION

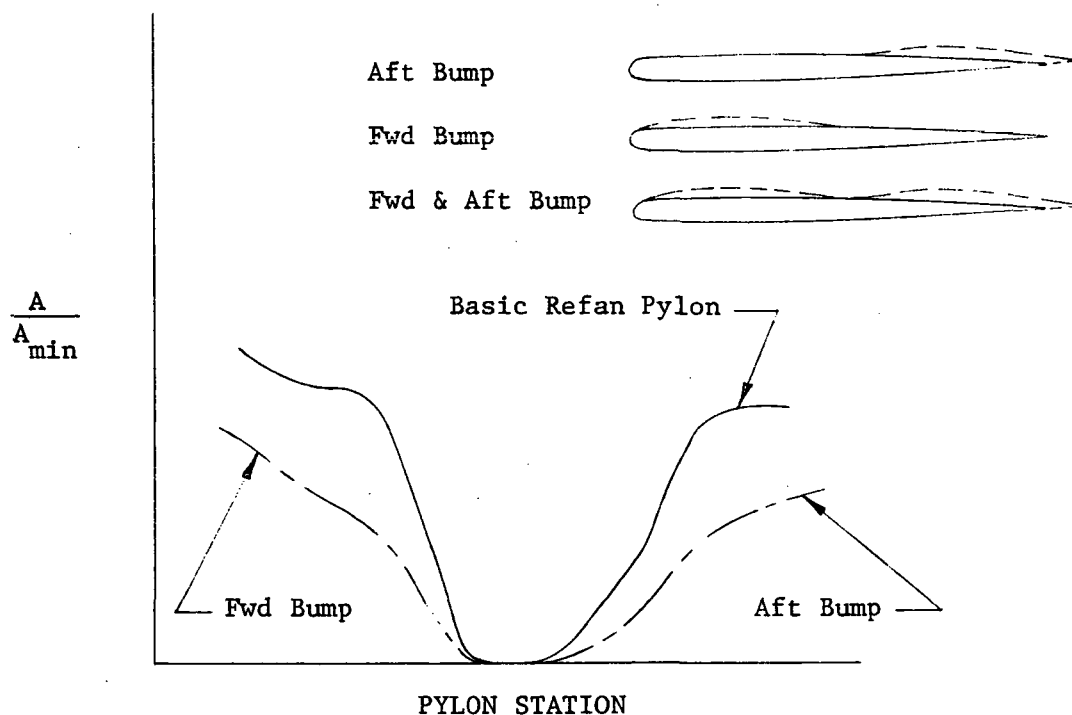
To determine the feasibility of a common long-duct refan-engine nacelle for all DC-8 models, serious consideration must be given to the aerodynamic design of the pylons for minimum interference drag. Previous wind tunnel and flight experience (e.g. Reference 1) has shown that the cruise drag is extremely sensitive to the placement of the nacelles and pylons on the wing. The potential interference penalties that can occur are related to the local Mach numbers in the channel formed by the wing, pylon, and nacelle and are manifested as a wave drag associated with shocks in the channel and/or as a drag associated with a thickening and possible separation of the boundary layer on the nacelle, pylon, or wing. The existing long-duct nacelle installation on the DC-8-62 and -63 and the short-duct nacelle installation on the Series 50 and 61 models are essentially interference-drag free installations. Since the long-duct nacelles on the Series 62 and 63 models are farther forward of the wing leading edge than the short-duct nacelles, the refan installation is not considered to be a problem on those aircraft. The long-duct refan nacelle installation on the Series 50 and 61 models, however, poses a potential problem. If the refan-engine were installed on the Series 50 and 61 as it is on the Series 62 and 63 (nacelle well out in front of the wing), reskinning of the wing would be required for flutter considerations. If, on the other hand, the long-duct refan nacelle were installed in the existing aft short-duct position, a significant interference drag might result. The reason for this concern can be seen from the sketch below, which presents a comparison of the wing-pylon-nacelle channel area distributions for the refan installation with those for





an interference-drag free installation and an installation with a significant interference penalty. The latter two area distributions are for similar installations that were previously tested. The area distribution for the installation with an interference penalty corresponds closely to the development of supersonic flow and shocks measured in the channel. It can be seen from the sketch that the convergence - divergence of the refan area distribution is worse than that of the interference-free installation.

As a result of this concern a high-speed wind tunnel test was conducted in the NASA Ames 11-foot transonic wind tunnel in January 1973 (Ames Test No. 11-703). The purpose of this test was to determine if an interference drag penalty existed for the long-duct refan nacelle installation on the existing Series 50 and 61 short-duct pylon, and, if necessary, to investigate potential fixes designed to minimize or eliminate the interference penalty. The potential fixes took the form of pylon bumps, which were designed to improve the channel area distribution shown in the sketch above. Three sets of modified pylons were designed and fabricated for this test. A sketch of the effect these pylons will have on the channel area distribution is presented below.



The pertinent results from this test are analyzed and discussed in this report.



### 3.0 SYMBOLS

$\frac{A}{A_{\min}}$	Ratio of local channel cross-section area to minimum value
$C_D$	Drag coefficient, $D/q_o S_w$
$\Delta C_D$	Incremental drag coefficient
$C_L$	Lift coefficient, $L/q_o S_w$
$C_p$	Pressure coefficient, $(P - P_o)/q_o$
$M$	Mach number
$p$	Static pressure, psf
$q$	Dynamic pressure, psf
$S_w$	Wing reference area, sq ft
$\eta$	Ratio of local semi-span station to total semi-span

#### SUBSCRIPTS

$L$	Local conditions
$o$	Free stream conditions



## 4.0 APPARATUS AND TEST

### 4.1 MODEL DESCRIPTION

#### 4.1.1 Basic Model

The model is a 3.429 percent scale representation of the DC-8 Series 50 aircraft and is designated LB-184R. The model was tested with the horizontal and vertical tail removed. The fuselage, wing, and baseline nacelles and pylons have been previously tested in the Ames facility. The refan nacelle and pylon configurations were fabricated for this test program. A photograph of the model installed in the Ames 11-foot transonic wind tunnel is presented in Figure 1.

#### 4.1.2 Nacelle Geometry

Because of the larger fan diameter of the JT3D-9 refan engine, the nacelle required to enclose the engine and accessories is also larger. The nacelle geometry is consistent with the maximum-treatment configuration shown in Reference 2. In order to retain the proper ground clearance most of the increased nacelle thickness is taken on the sides with larger kidney ducts, the exception being that some increased thickness is required on the forward upper cowl for angle of attack capability. The refan nacelle geometry has the following characteristics:

1. The inlet length from the engine face to the highlight is 47.8 inches.
2. The maximum nacelle width is 74.3 inches (plan view).
3. The overall nacelle length is 225.5 inches.
4. The nacelle is of long duct design.
5. The afterbody boattail angle is 13.5 degrees.
6. The inlet is canted down 4 degrees relative to the engine centerline to align it with the local flow angle at cruise conditions.

Since it is impossible to correctly simulate the short-duct fan flow of the production DC-8-50 and -61 nacelles with flow through nacelles, another set of JT3D long-duct nacelles was used as the baseline configuration for this test. A dimensional sketch of the refan nacelle compared to the baseline nacelle is presented in Figure 2.



#### 4.1.3 Nacelle Installation Comparison

The refan-engine nacelle installation is compared to the DC-8-50 and -61 production short-duct nacelle installation in Figure 3. The proposed refan pylon has been designed to be compatible with the existing short-duct pylon structural box and with the existing pylon foot-print on the wing upper and lower surface (i.e. the refan pylon is a minimum structural change short-duct pylon). The refan pylon trailing edge extends beyond the existing pylon trailing edge because of the difference in thrust reverser mechanisms for the two installations. The bump on the leading edge of the refan pylon would be required to house a heat exchanger for the cabin airconditioning system.

The baseline set of JT3D long-duct nacelles is mounted on contoured pylons in an aft position like the refan nacelles and has been found from previous wind tunnel and flight testing to be an essentially interference-drag free installation. A comparison of the baseline and refan nacelle installations is presented in Figure 4.

#### 4.1.4 Pylon Modifications

Three sets of modified pylons were designed and fabricated in an attempt to minimize or eliminate any potential interference drag penalty resulting from the basic refan nacelle installation. The pylons were designed to improve the channel area distribution (see the sketch on page 4). The modifications took the form of forward and aft bumps on the inboard side of the inboard and outboard pylons. Figure 5 presents a comparison between the basic refan pylons and the modified pylons. The three pylon sets consist of the forward and aft bumps individually and in combination.

### 4.2 TEST APPARATUS

#### 4.2.1 Facility and Model Installation

The NASA Ames Research Center 11- by 11-foot continuous flow variable density transonic wind tunnel was used for this test program.

The model was mounted on a 2.5-inch diameter internal strain gage balance and installed on the Ames straight sting No. 9797-D3-6 which was mated to the Ames straight sting No. 9797-D4-1. This assembly was inserted into the Ames straight



adapter, with 40-inch extension, which was then mounted on the pitch pod. The balance cavity in the fuselage center body is at a five degree angle to the fuselage reference plane, such that, when the model is at zero angle of attack, the balance is at +5.0 degrees angle of attack.

The model was aligned in pitch and roll by means of leveling bubbles in the pitch and roll planes embedded in the fuselage centerbody.

A drawing of the actual model installation is presented in Figure 6.

#### 4.2.2 Instrumentation

The force data were gathered with a six-component Mark XIA internal strain gage balance and the pressure data were gathered with a six-valve scanivalve module. The model angle of attack was measured by an analog signal conditioner in the wind tunnel control room. This electronic device was connected to the balance normal force gages and accounted for sting bend and balance deflections, thus allowing the tunnel operator to set the desired angle. The model support sting was instrumented to indicate contact between the fuselage and sting. No contact was indicated throughout the test.

The location of the static pressure orifices is shown in Figure 7. There are four rows of pressures in the inboard channel of each nacelle and two in the outboard channel plus one row on the wing upper surface on the inboard side of each nacelle. This instrumentation is common to all configurations.

All forces, moments and pressures were recorded on the Ames wind tunnel data acquisition system.

#### 4.3 TEST PROCEDURE AND DATA ACCURACY

The test was conducted at a constant Reynolds number of 7 million per foot ( $5.5 \times 10^6$  on the mean aerodynamic chord) through a Mach number range from 0.70 to 0.84. The Reynolds number was held to within  $\pm 100,000$  and the Mach number to within  $\pm 0.002$  of the specified values. The full Reynolds number capability, 8 million per foot, was not utilized, because of the concern about sting divergence at the higher dynamic pressures. Angle of attack was varied



at each Mach number in one-half degree increments over a range corresponding to lift coefficients between zero and 0.5. The angle of attack tolerance is  $\pm 0.1$  degree of the indicated value. Selected Mach numbers were repeated to ensure the validity of the data. The data repeatability was excellent throughout the test ( $C_D$  repeated within  $\pm 0.0001$ ). The pressure data were gathered at enough Mach numbers to provide the necessary information for understanding any potential interference problems. All data were gathered with the horizontal and vertical tails removed.



## 5.0 RESULTS AND DISCUSSION

### 5.1 BASIC REFAN INSTALLATION

The incremental drag difference between the refan-engine nacelle installation and the essentially interference-drag free baseline installation is presented in Figure 8. It can be seen that, within the data scatter, there is a drag penalty of about two drag counts ( $\Delta C_D = 0.0002$ ) for the refan installation, which is independent of Mach number and lift coefficient. About a quarter of this penalty can be accounted for by the basic parasite drag difference between the isolated nacelles and pylons. The remaining excess or interference drag for the refan installation is thus less than 1.5 drag counts (1/2% of total cruise drag). The magnitude of the interference drag and the fact that it is independent of Mach number and lift coefficient suggests that this small penalty is not a result of a wave drag and/or a boundary layer separation associated with shocks in the wing-pylon-nacelle channel, as was originally feared from examination of the channel area distributions, but probably results from a general thickening in the boundary layer of some of the components when they are integrated. Analysis of the pressure data somewhat substantiates this conclusion.

Figures 9 and 10 present the refan nacelle, pylon, and wing pressure distributions compared with the baseline distributions for the inboard and outboard installations at a typical cruise condition ( $M_0 = 0.82$ ,  $C_L = 0.4$ ). It can be seen in Figure 9 that there is a local region of supersonic flow which extends across the inboard channel of the inboard installation, but does not extend down around to the maximum half breadth of the nacelle. The flow in the remaining three channel areas (outboard channel of inboard nacelle installation, Figure 9, and both inboard and outboard channels of outboard nacelle installation, Figure 10) is almost entirely free of any supersonic flow.

The effect of Mach number on the channel pressure distributions is presented in Figure 11, where it can be seen that there is no supersonic flow in the wing-pylon-nacelle channels at  $M_0 = 0.70$ . The fact that the interference drag penalty shown in the force data (Figure 8) is independent of Mach number would indicate that the local region of supersonic in the inboard channel of the inboard nacelle installation at  $M = 0.82$  is not sufficient to cause any wave drag.



The effect of lift coefficient on the channel pressure distributions is presented in Figure 12 for  $M_0 = 0.82$ . The maximum local Mach number in the inboard channel of both the inboard and outboard nacelle installations is slightly higher at 0.3 lift coefficient than it is at 0.4. Again, reference to the force data (Figure 8) would indicate that this slight increase in local Mach number at the lower lift coefficient is not sufficient to cause any wave drag.

A comparison of the wing upper surface pressure distributions for the two nacelle installations is presented in Figure 13. The pressure distributions are almost identical at both .7 and .82 Mach number.

The very small interference drag penalty (1/2% of total cruise drag) measured in this test for the installation of the long-duct refan nacelle on the existing (minimum structural change) Series 50 and 61 short-duct pylon would be more than off-set by the large improvement of a long-duct nacelle over a short-duct nacelle. This improvement has been demonstrated on the existing DC-8 (Series 50 and 61 models compared to Series 62 and 63 models).

## 5.2 PYLON MODIFICATION

Three sets of modified pylons were designed and fabricated for this test. As mentioned previously, the purpose of these pylons was to minimize or eliminate any potential interference drag resulting from shock waves in the wing-pylon-nacelle channel by improving the channel area distributions (see the sketches on pages 3 and 4). Since the on-line force-data analysis at the wind tunnel indicated that the interference drag for the basic refan nacelle installation was quite small, only one of the modified pylons was tested.

Figure 14 presents the incremental drag difference between the refan installation with the basic pylon and with the modified pylon having only the aft-bump. It can be seen that within the data scatter, there is a drag penalty of over two drag counts (almost 1% of total cruise drag) for the modified pylon. In view of the fact that the basic refan installation is free of shock-related interference drag, this result is not surprising. Since the improved area distribution feature of the bump is not required, it has apparently become a source of additional parasite drag.



## 6.0 CONCLUSIONS

A high-speed wind tunnel test was conducted in the NASA Ames 11-foot facility in support of the NASA refan program in order to assess the effect on cruise performance of installing a long-duct refan-engine nacelle on the DC-8-50 and -61. Analysis of the results from this test leads to the following conclusions:

1. At a typical cruise condition there exists an interference drag penalty of less than one-percent total cruise drag for the installation of the long-duct refan nacelle on the existing (minimum structural change) Series 50 and 61 short-duct pylon. This very small penalty would, however, be much more than off-set by the large improvement, demonstrated on the existing DC-8, of a long-duct nacelle over a short-duct nacelle.
2. At cruise conditions some supersonic flow is present in the inboard channel of the inboard refan-nacelle installation, but it is not sufficient to cause any wave drag or boundary layer separation. The small interference drag results from a general thickening in the boundary layer of some of the components when they are integrated.
3. The one pylon modification tested resulted in a drag penalty, because its design goal of eliminating shock-related interference drag was not required and this bump thus became a source of additional parasite drag.
4. From aircraft performance considerations, a common long-duct refan-engine nacelle is certainly feasible for all DC-8 models.



## 7.0 REFERENCES

1. Kutney, John T. and Piszkin, Stanley P.: Reduction of Drag Rise on the Convair 990 Airplane. J. Aircraft Vol. 1 No. 1, Jan - Feb 1964.
2. Anonymous: Program on Ground Test of Modified Quiet Clean JT3D and JT8D Engines in their respective nacelles. DC-8-61 Engine and Nacelle/Airframe Integration Definition. Douglas Report MDC J5731, 10 November 1972.



**Page Intentionally Left Blank**



## 8.0 FIGURES

<u>FIGURE NO.</u>	<u>TITLE</u>
1.	Photo of model installation
2.	Nacelle geometry
3.	Long-duct refan-engine nacelle installation compared to DC-8-50/61 production installation
4.	Long-duct refan-engine nacelle installation compared to test program baseline installation
5.	Basic refan pylons compared to modified pylons
6.	Model installation drawing
7.	Location of static pressure orifices
8.	Incremental drag difference between refan and baseline nacelle installations
9.	Refan channel pressure distributions compared to baseline-inboard nacelle
10.	Refan channel pressure distributions compared to baseline-outboard nacelle
11.	Effect of Mach number on refan channel pressure distributions
12.	Effect of lift coefficient on refan channel pressure distributions
13.	Effect of refan installation on wing upper surface pressure distributions
14.	Incremental drag due to addition of aft-bump to basic refan pylon



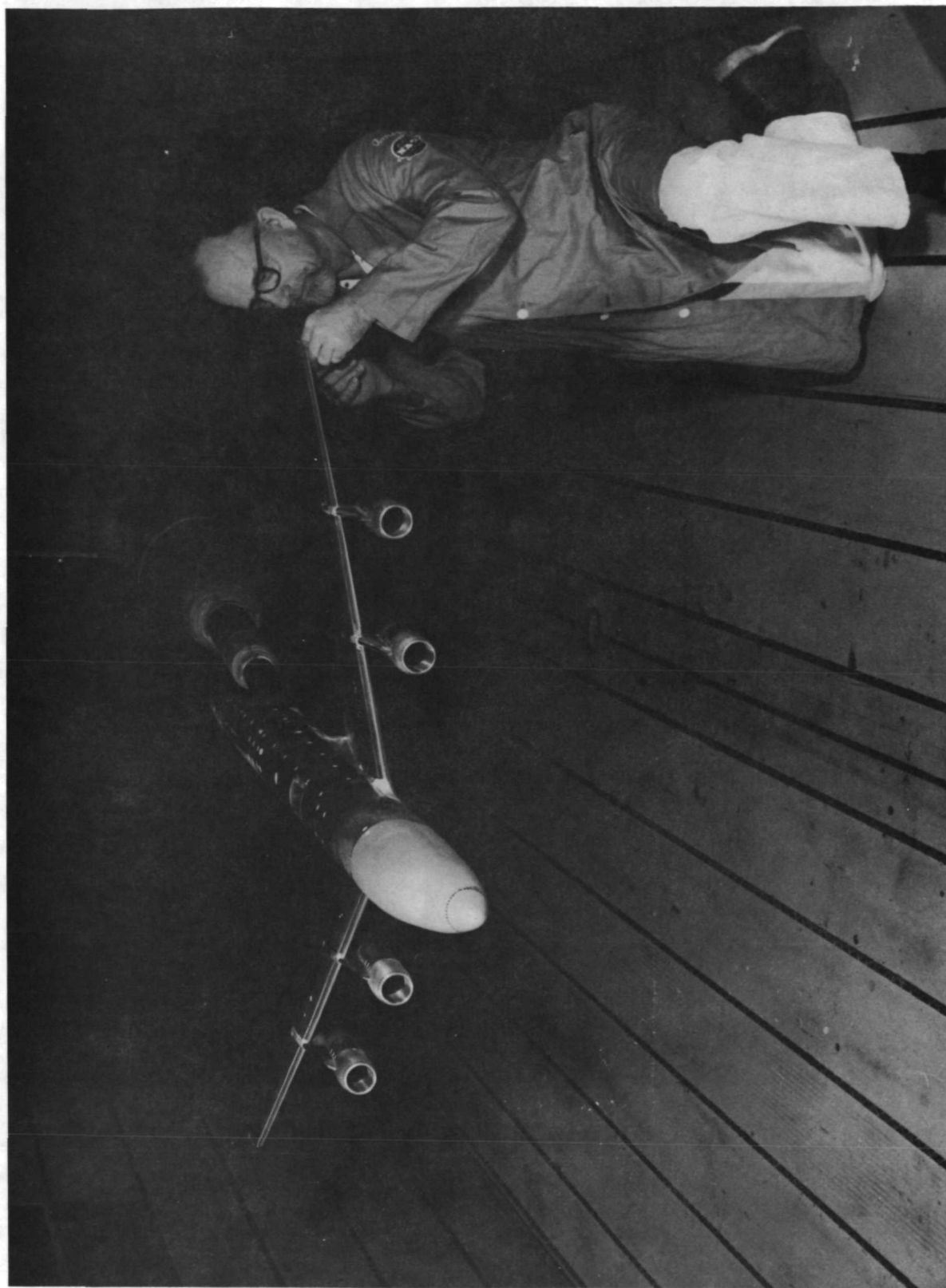


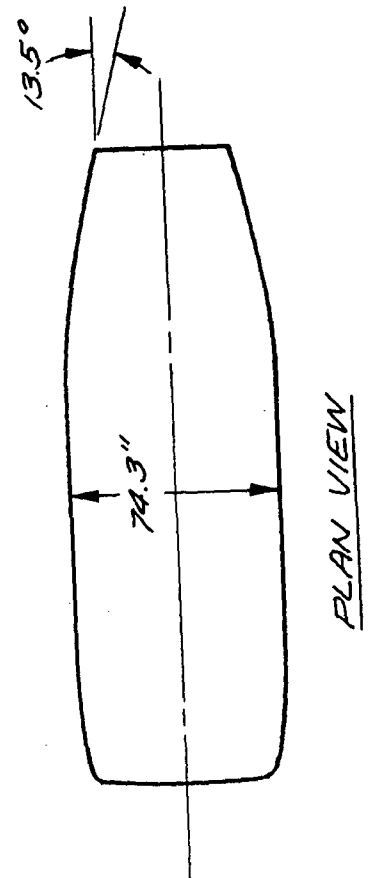
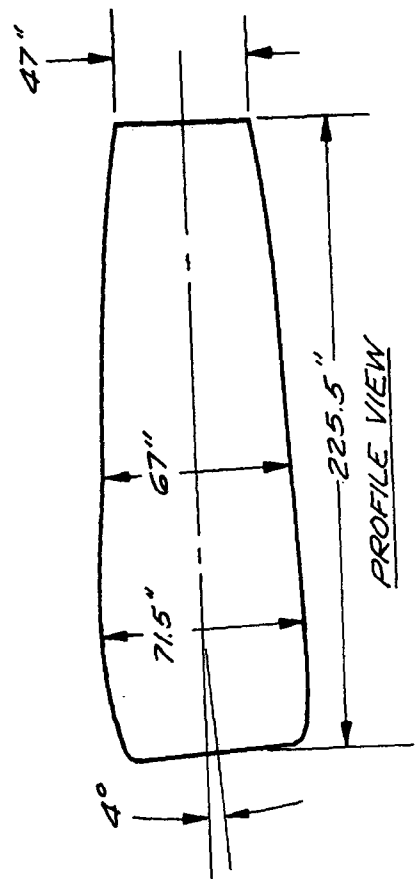
Figure 1.- Photo of model installation.



Page Intentionally Left Blank



REFAN NACELLE (JT3D-9)



BASELINE NACELLE (JT3D-3B)

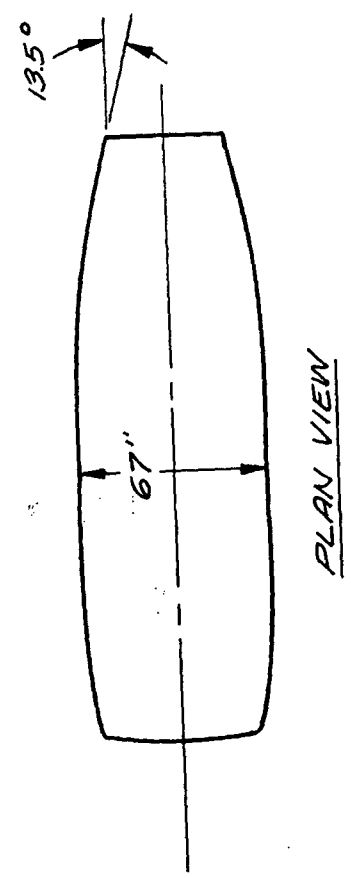
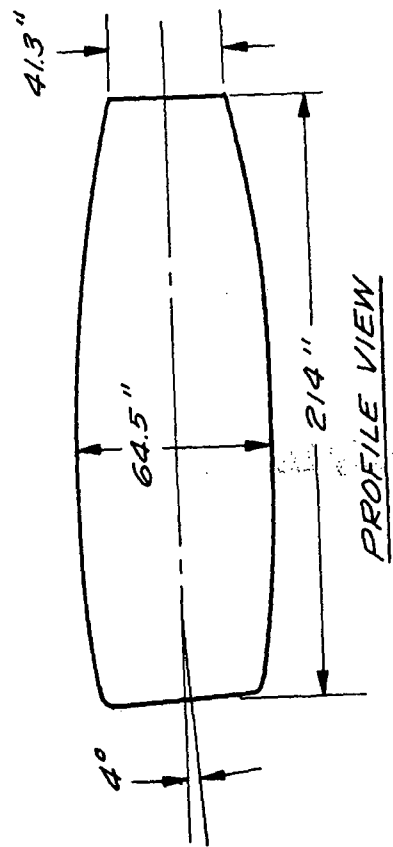
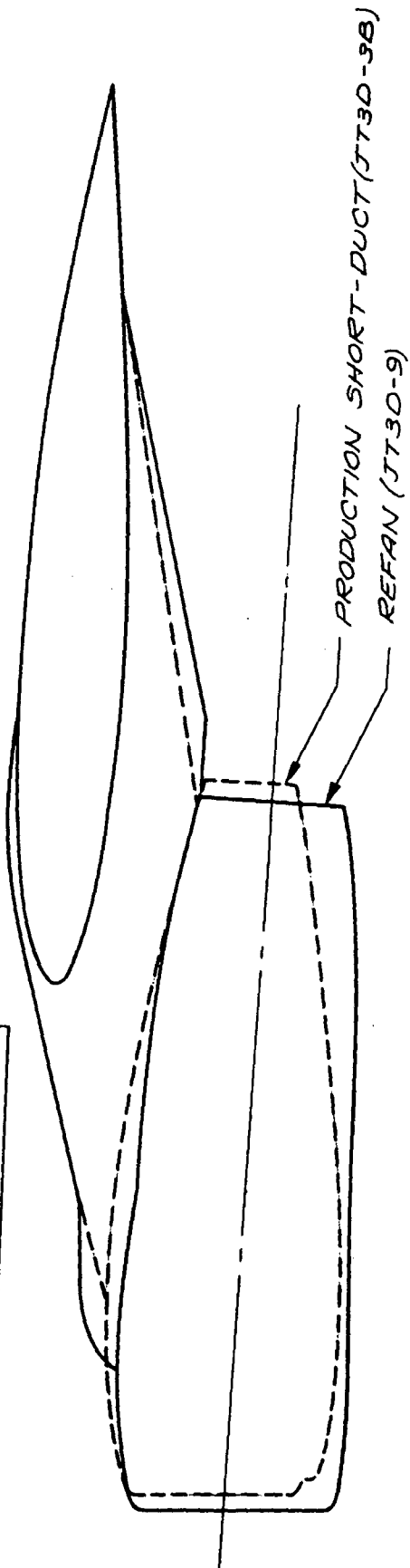


FIGURE 2: NACELLE GEOMETRY



# INBOARD NACELLE INSTALLATION



# OUTBOARD NACELLE INSTALLATION

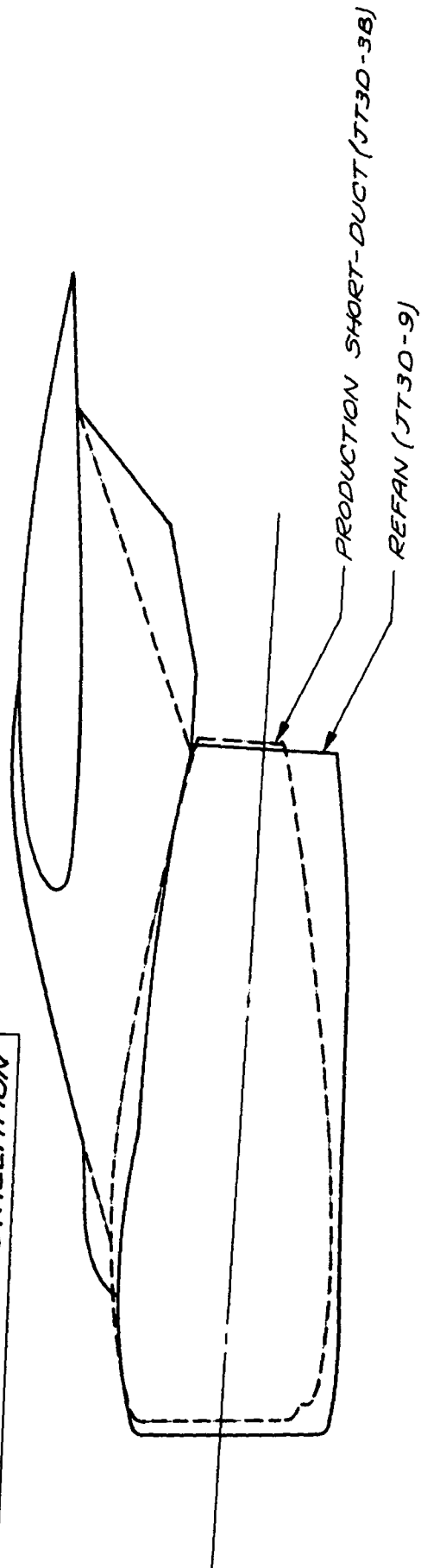


FIGURE 3 : LONG-DUCT REFAN-ENGINE NACELLE INSTALLATION COMPARED TO DC-8-50/61  
PRODUCTION INSTALLATION



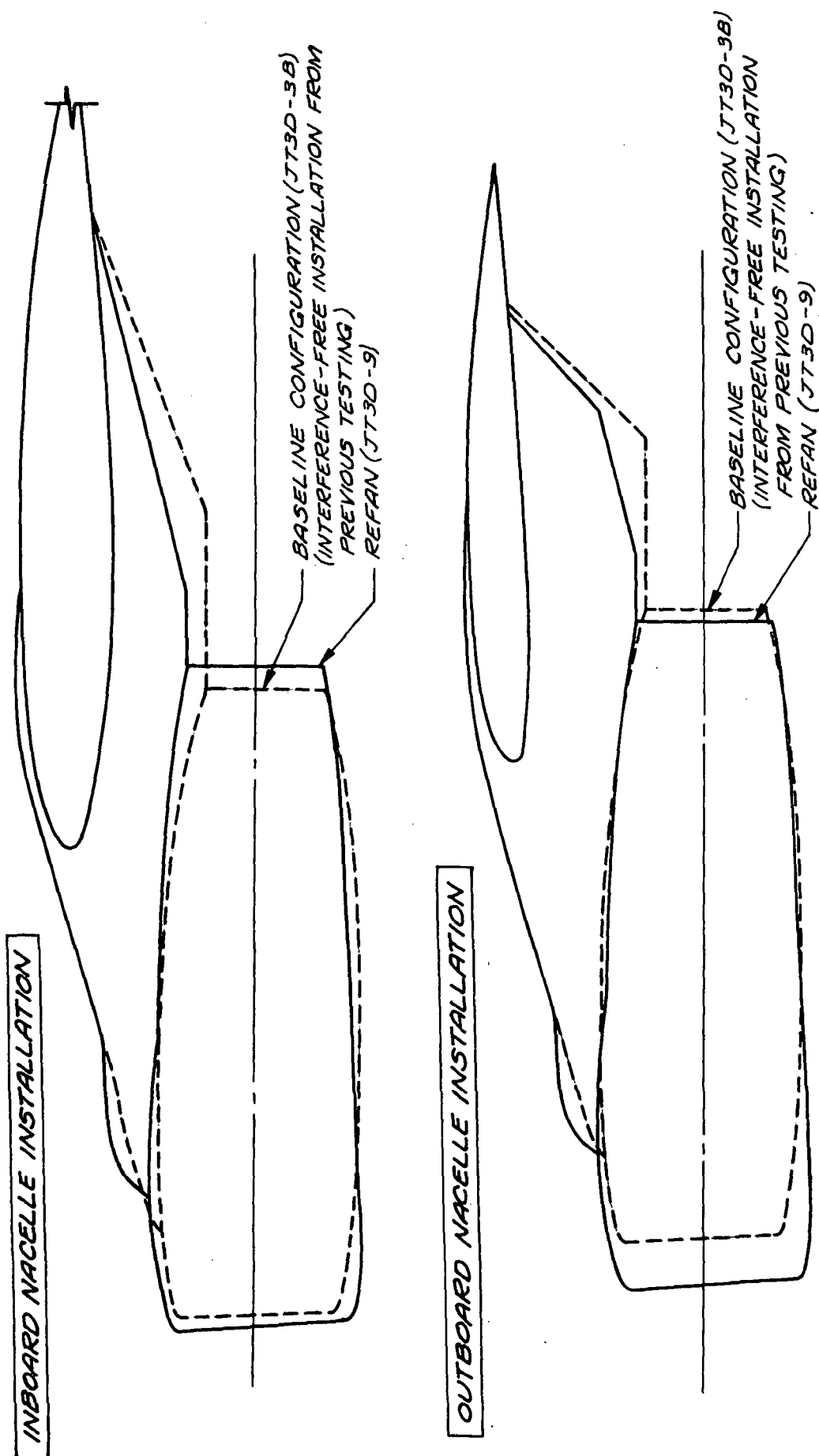
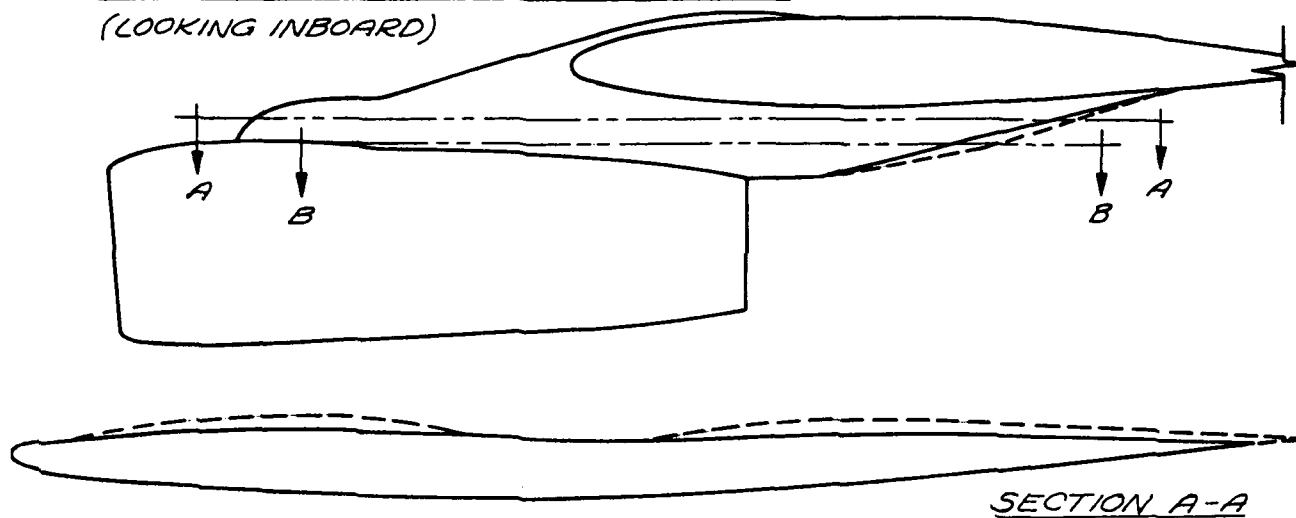


FIGURE 4 : LONG-DUCT REFAN-ENGINE NACELLE INSTALLATION COMPARED TO TEST PROGRAM  
BASELINE INSTALLATION



# **INBOARD NACELLE INSTALLATION**

(LOOKING INBOARD)



NOTE: DASHED CONTOURS REPRESENT REFAN PYLON MODIFICATIONS.

# **OUTBOARD NACELLE INSTALLATION**

(LOOKING INBOARD)

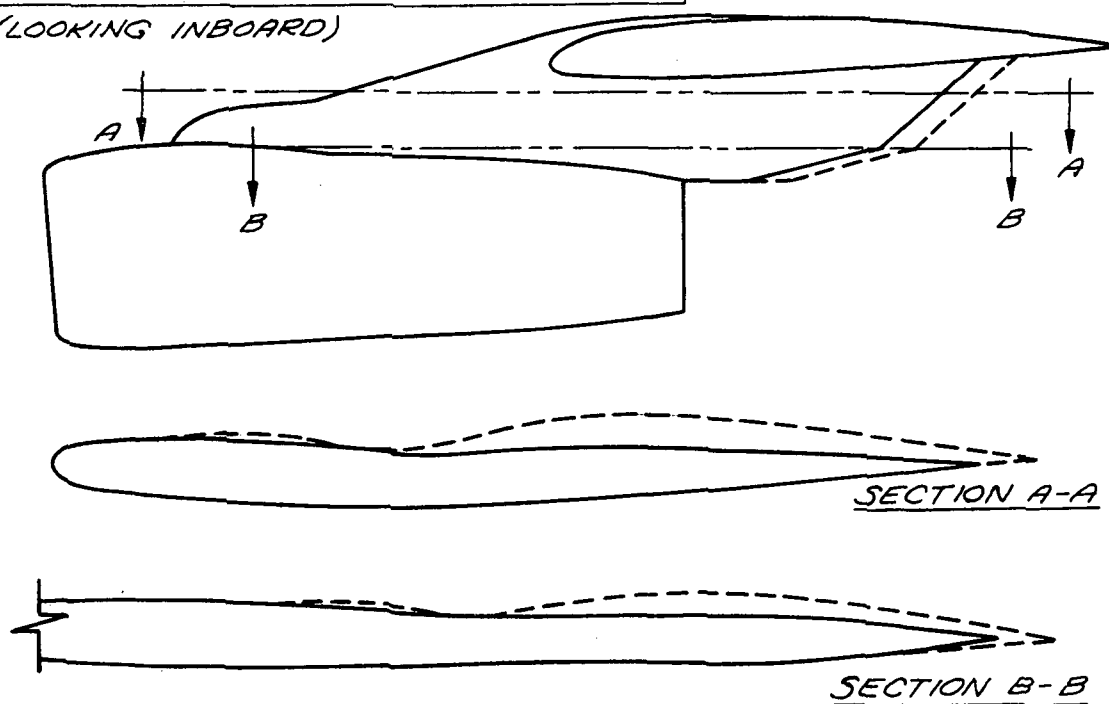


FIGURE 5 : BASIC REFAN PYLONS COMPARED TO MODIFIED PYLONS



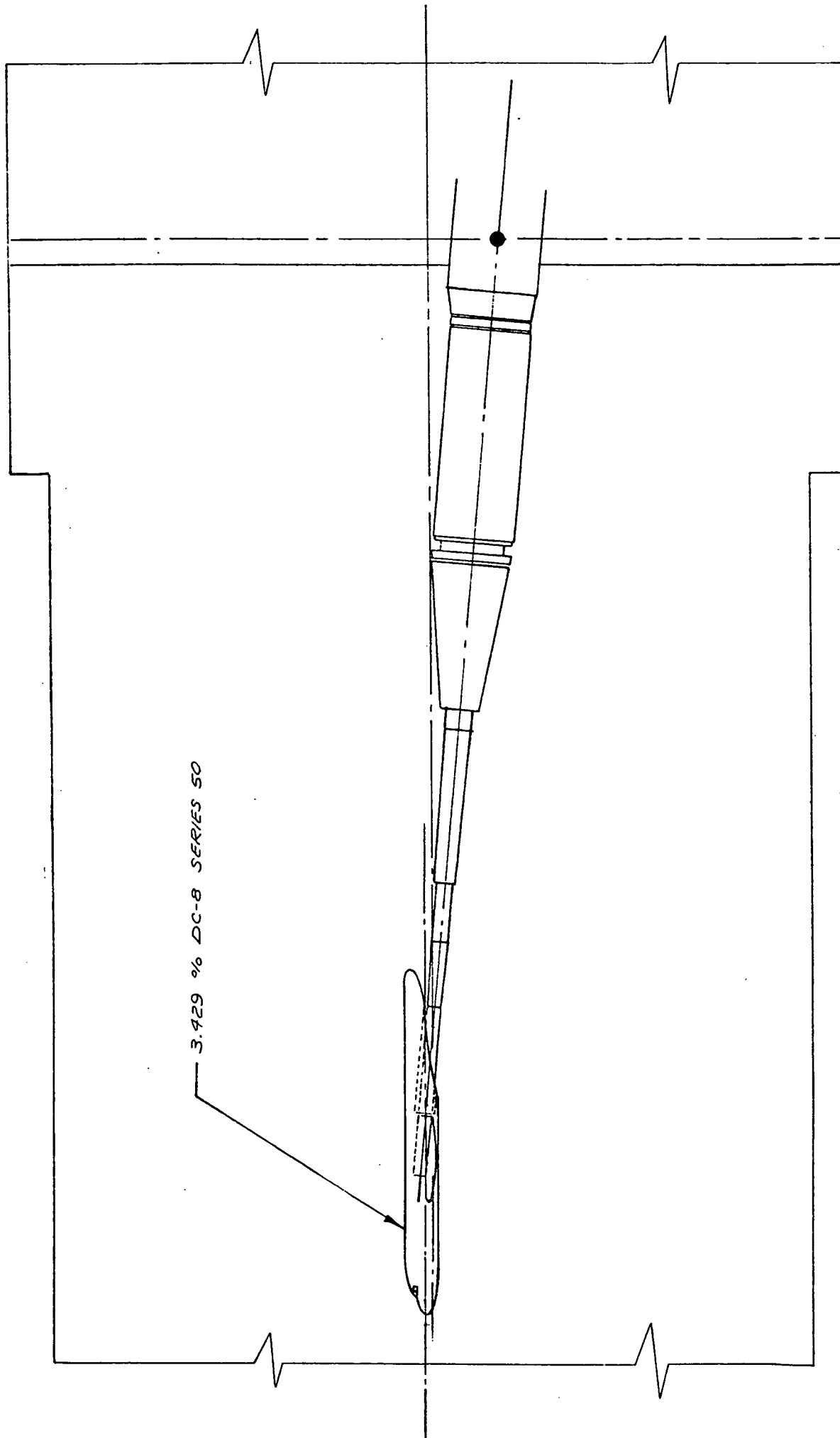
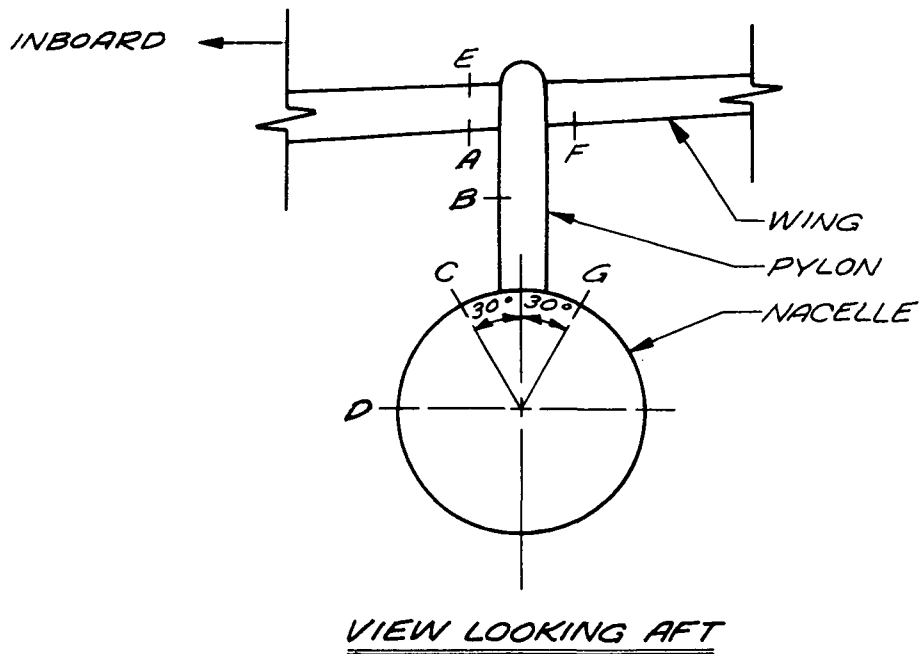


FIGURE 6: MODEL INSTALLATION DRAWING





ROW	NUMBER OF PRESSURE ORIFICES PER ROW	
	INBOARD NACELLE	OUTBOARD NACELLE
A	23 ( $\eta = .347$ )	23 ( $\eta = .611$ )
B	15	13
C	10 (BASELINE NACELLE) 12 (REFAN NACELLE)	9
D	10	9
E	19 ( $\eta = .347$ )	20 ( $\eta = .611$ )
F	23 ( $\eta = .375$ )	23 ( $\eta = .641$ )
G	7	7

FIGURE 7 : LOCATION OF STATIC PRESSURE ORIFICES



NOTE: STRAIGHT LINE FAIRING THROUGH DATA  
REPRESENTS AVERAGE OF ALL DATA  
INDEPENDENT OF  $M$  &  $C_L$

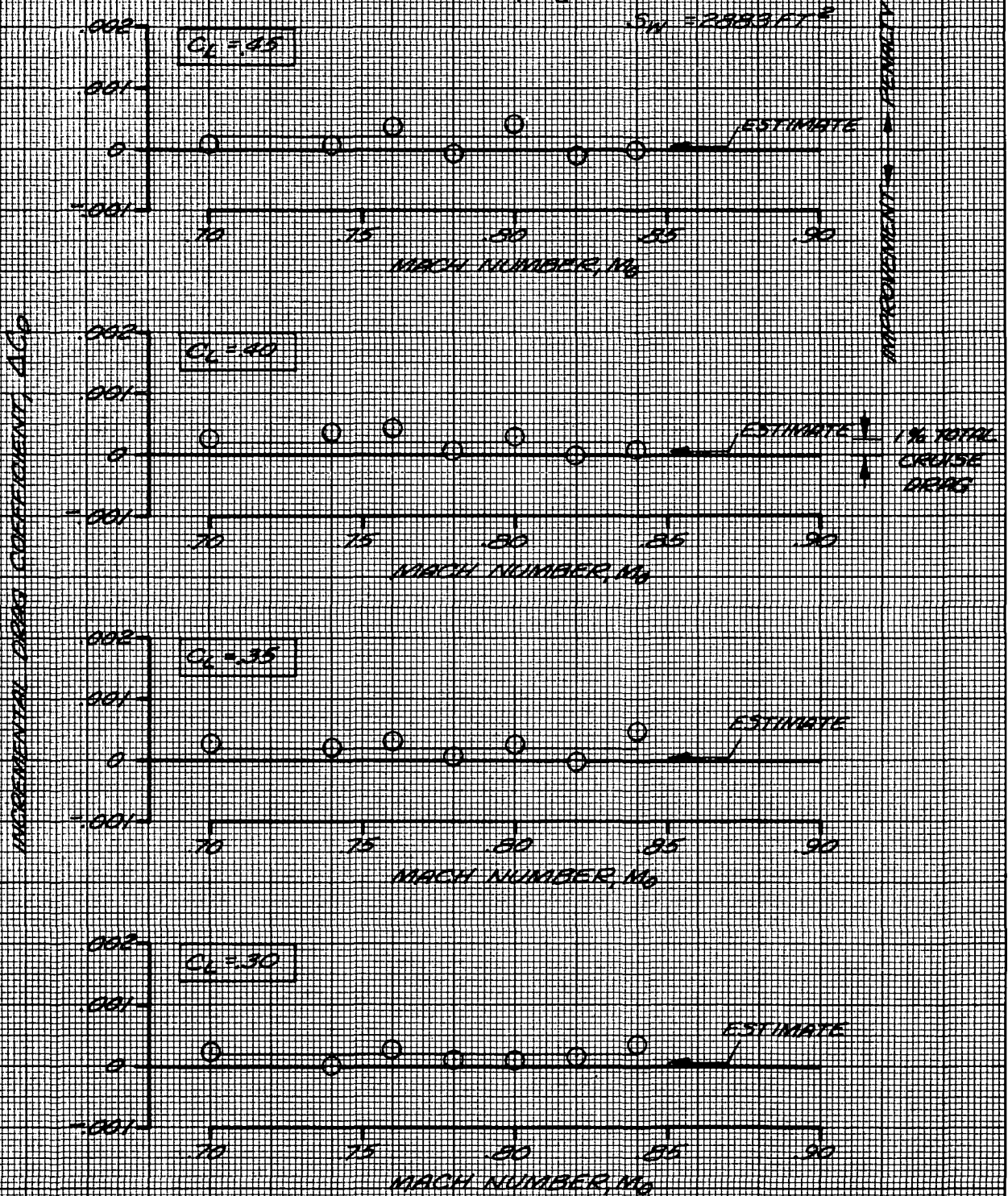


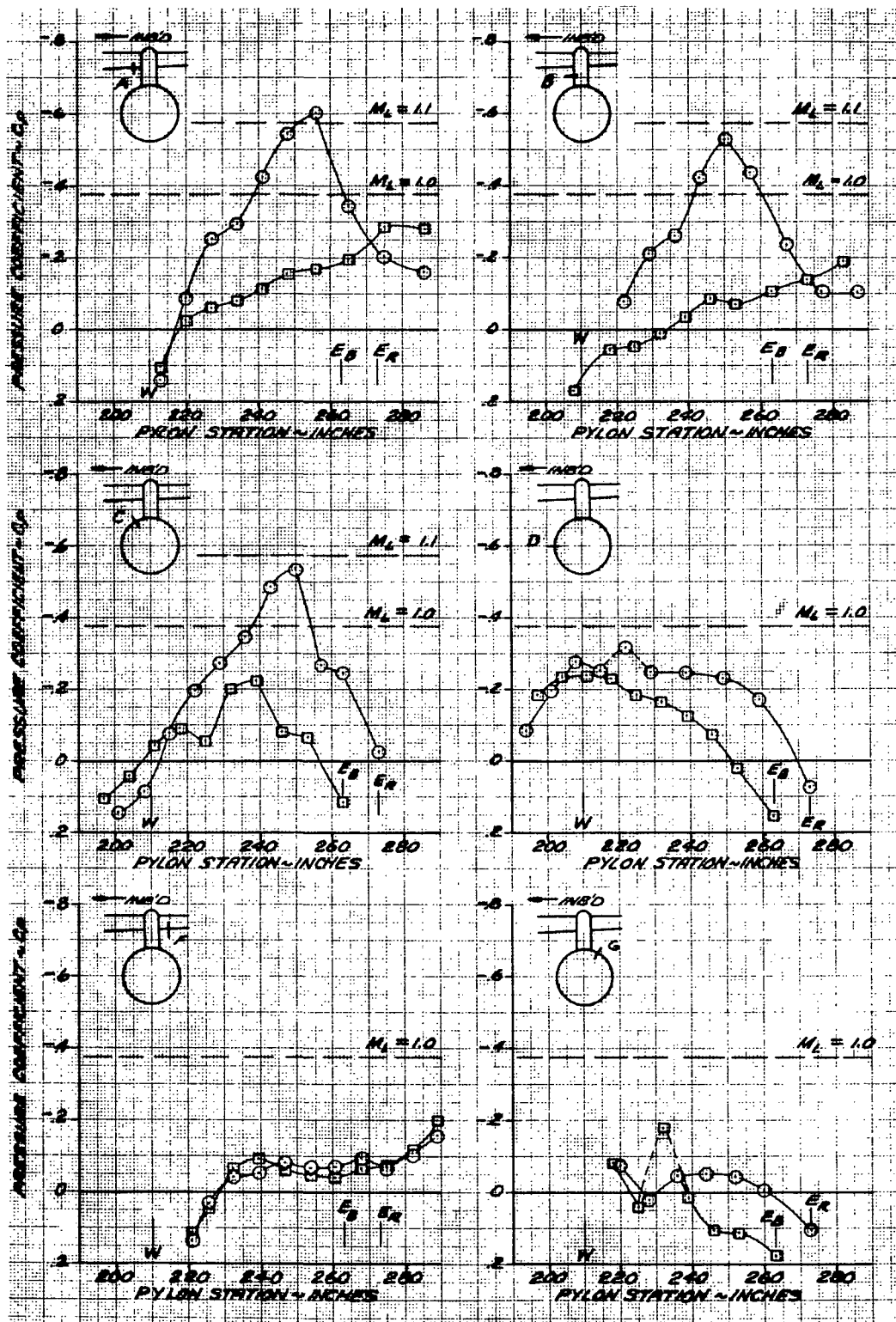
FIGURE B: INCREMENTAL DRAG DIFFERENCE BETWEEN RETAIN  
AND BASELINE NACELLE INSTALLATIONS.



SYM	CONFIGURATION
○	REFAN
□	BASLINE

$M_0 = .82, C_L = .40$

CODE	LOCATION OF:
W	INTERSECTION OF WING L.E. AND PYLON $C_L$ IN PLAN VIEW
$E_B$	BASELINE NACELLE EXIT
$E_R$	REFAN NACELLE EXIT



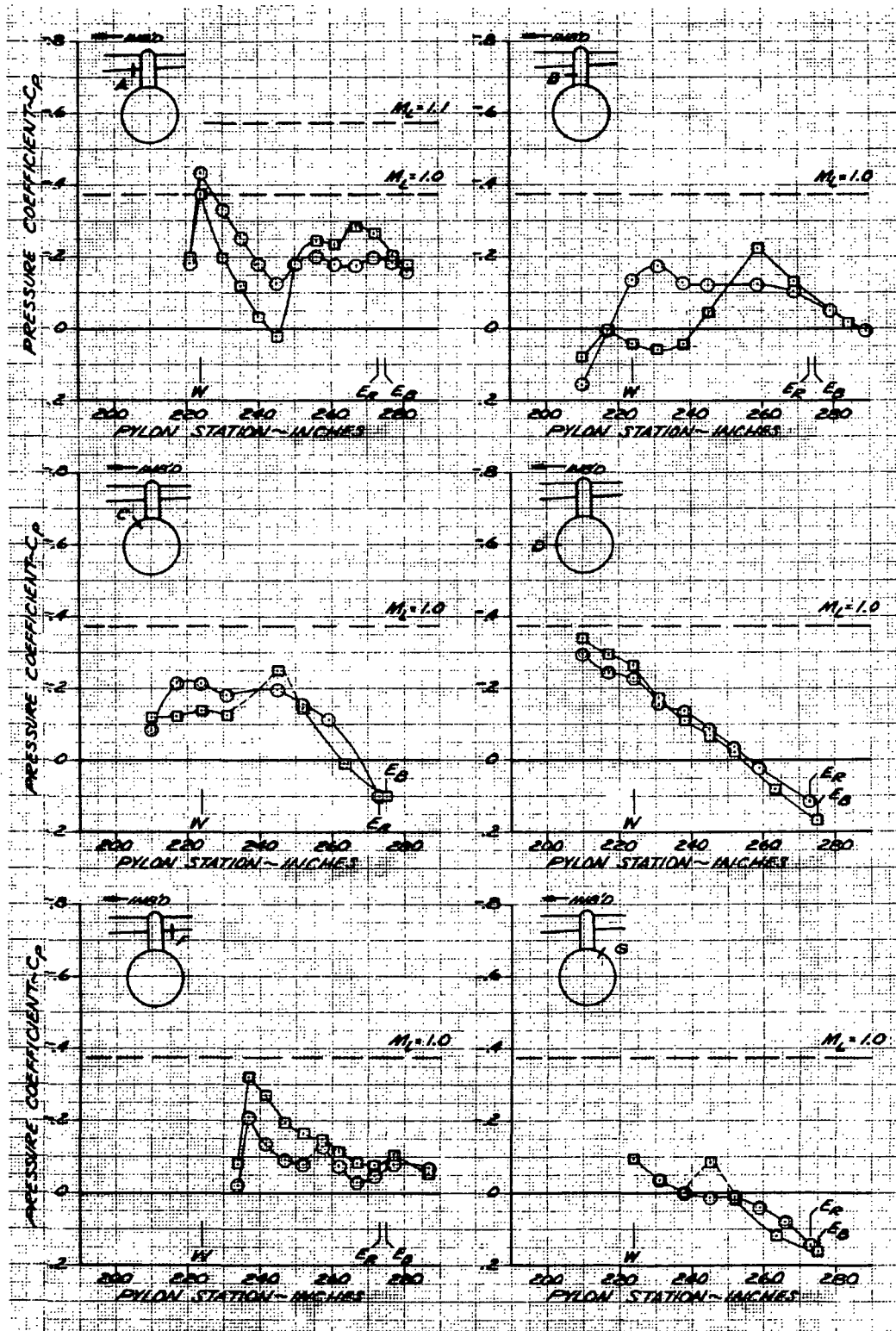
REFAN CHANNEL PRESSURE DISTRIBUTIONS COMPARED TO BASELINE-INBOARD NACELLE  
FIGURE 9



SYM	CONFIGURATION
○	REFAN
□	BASILINE

$M_0 = 0.82, C_L = .40$

CODE	LOCATION OF:
W	INTERSECTION OF WING L.E. AND PYLON $\xi$ IN PLAN VIEW
$E_B$	BASILINE NACELLE EXIT
$E_R$	REFAN NACELLE EXIT



REFAN CHANNEL PRESSURE DISTRIBUTIONS COMPARED TO BASELINE - OUTBOARD NACELLE  
FIGURE 10



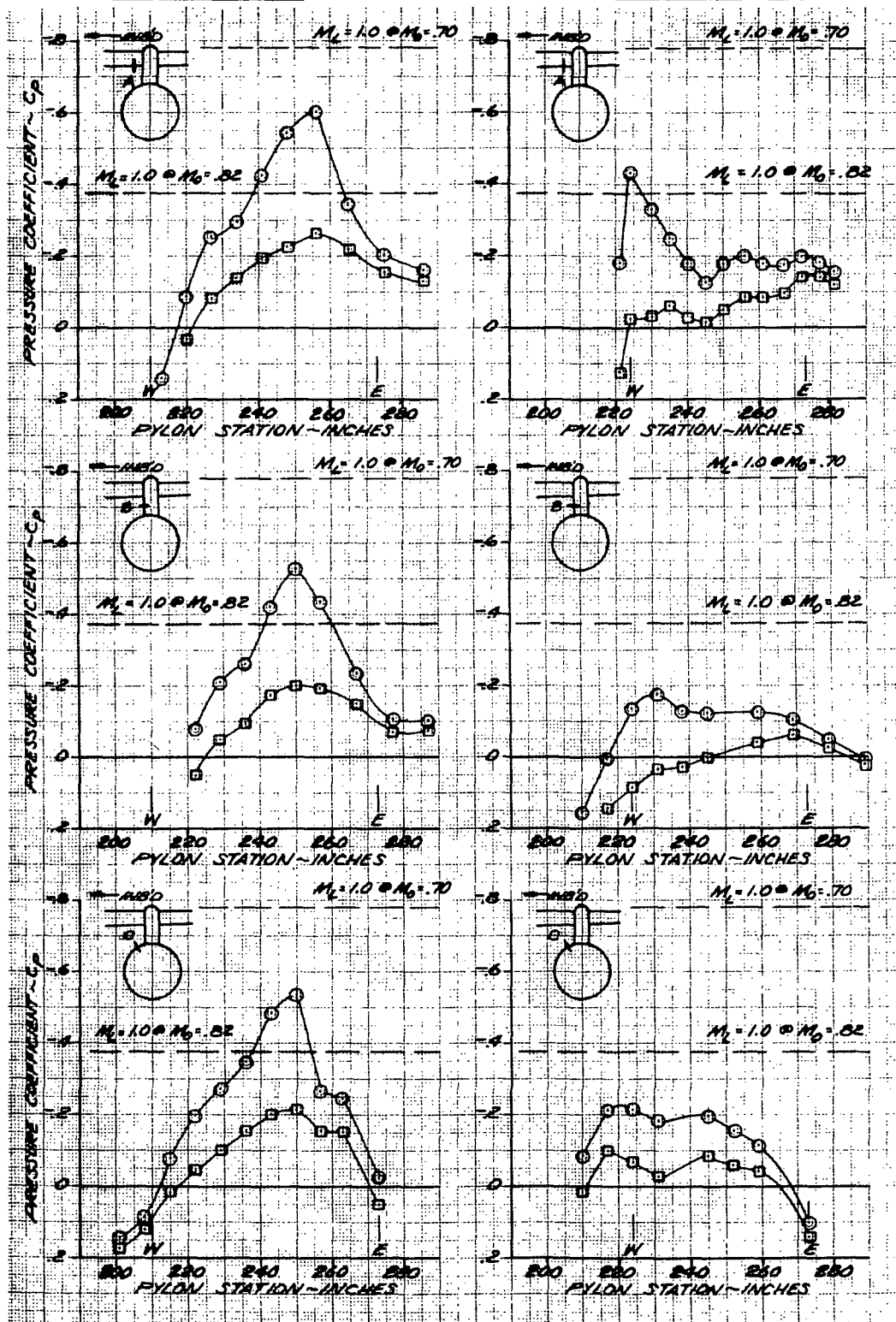
SYM.	MACH NUMBER
○	.82
□	.70

$$C_L \approx .40$$

CODE	LOCATION OF:
W	INTERSECTION OF WING L.E. AND PYLON $\xi$ IN PLAN VIEW
E	NACELLE EXIT

### INBOARD NACELLE

### OUTBOARD NACELLE



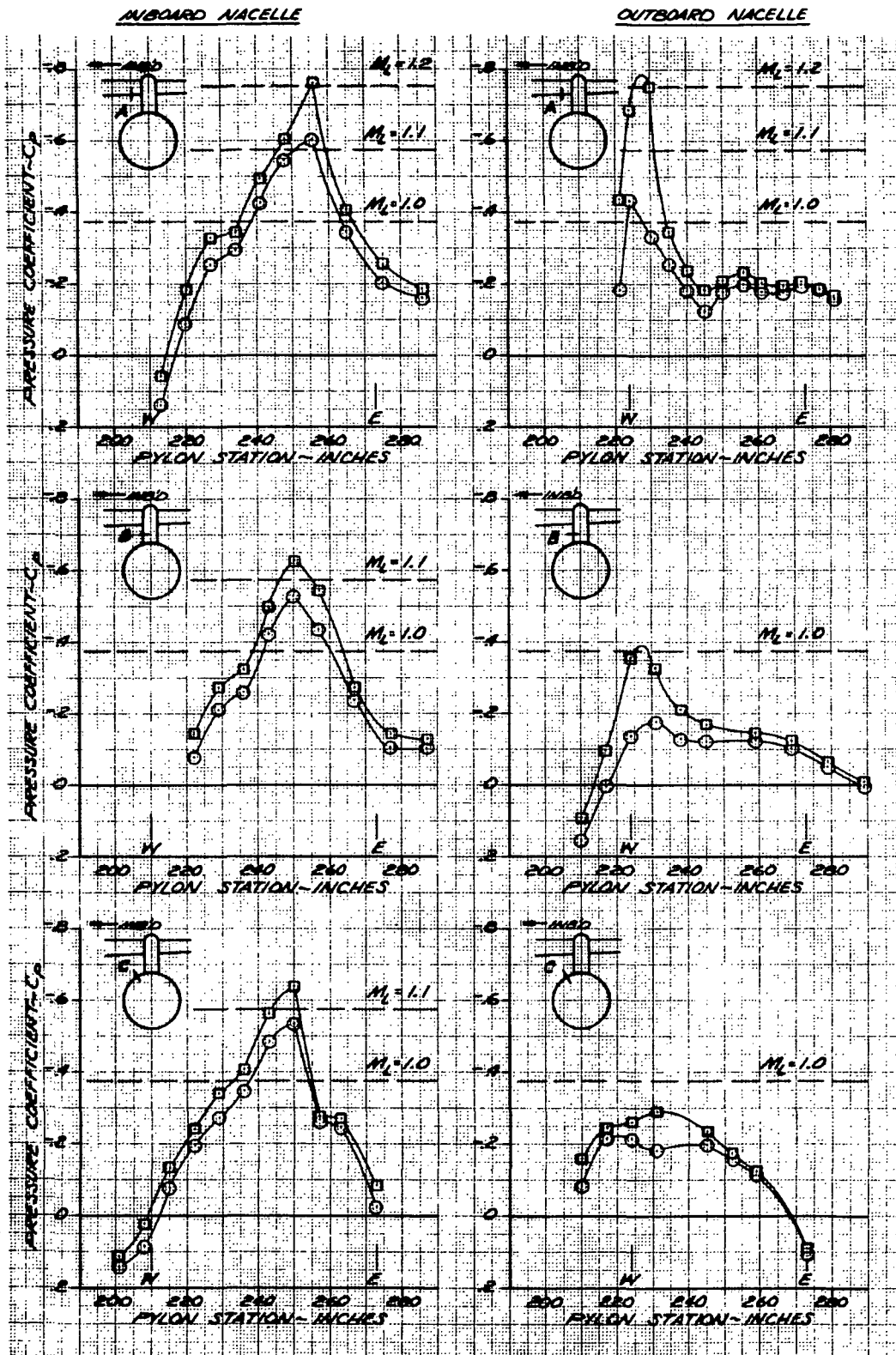
EFFECT OF MACH NUMBER ON REFAN CHANNEL PRESSURE DISTRIBUTIONS  
FIGURE 11



SYM	LIFT COEFFICIENT
○	.4
□	.3

$M_0 = .82$

CODE	LOCATION OF:
W	INTERSECTION OF WING L.E. AND PYLON $\xi$ IN PLAN VIEW
E	NACELLE EXIT





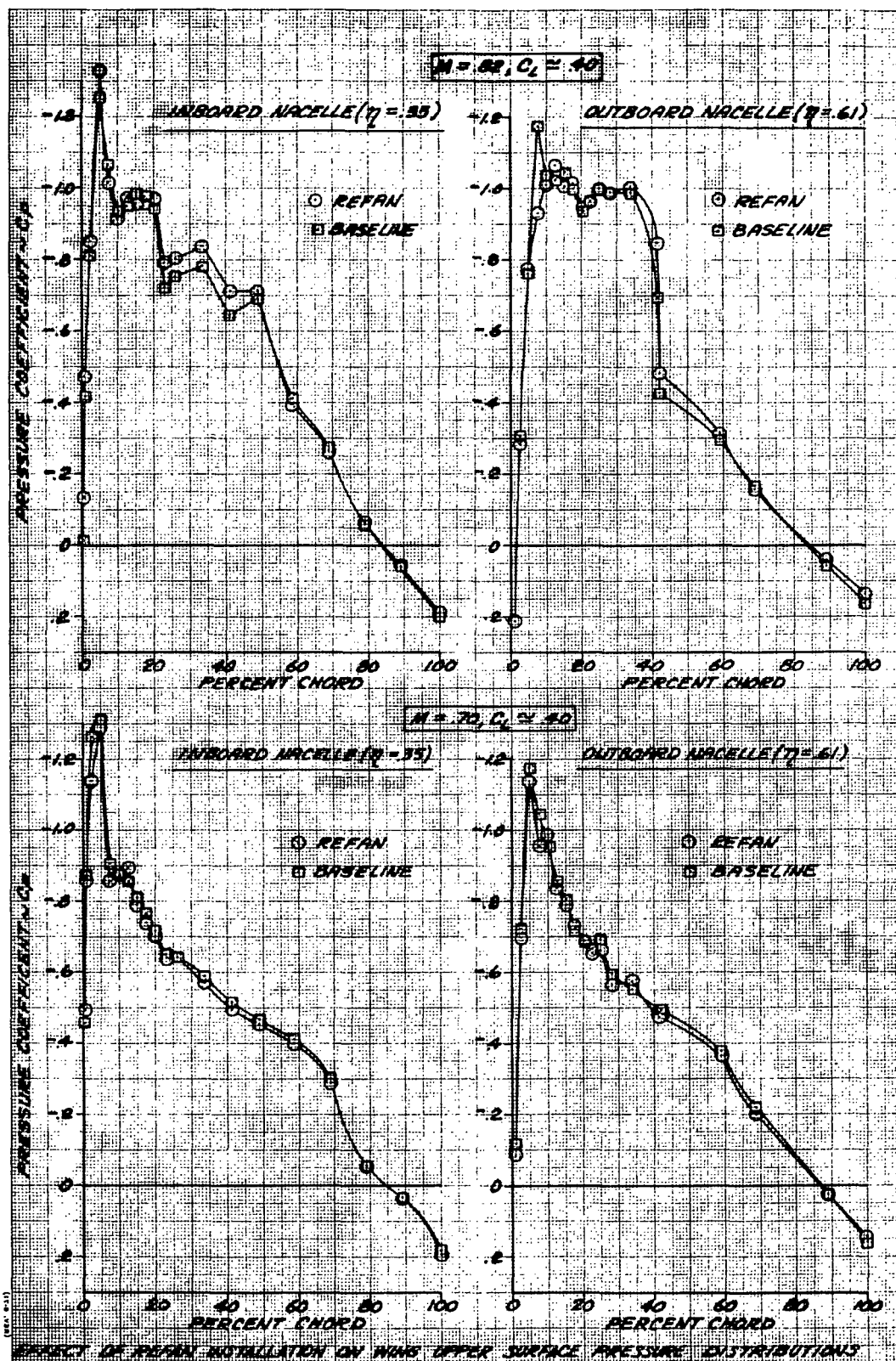


FIGURE 13



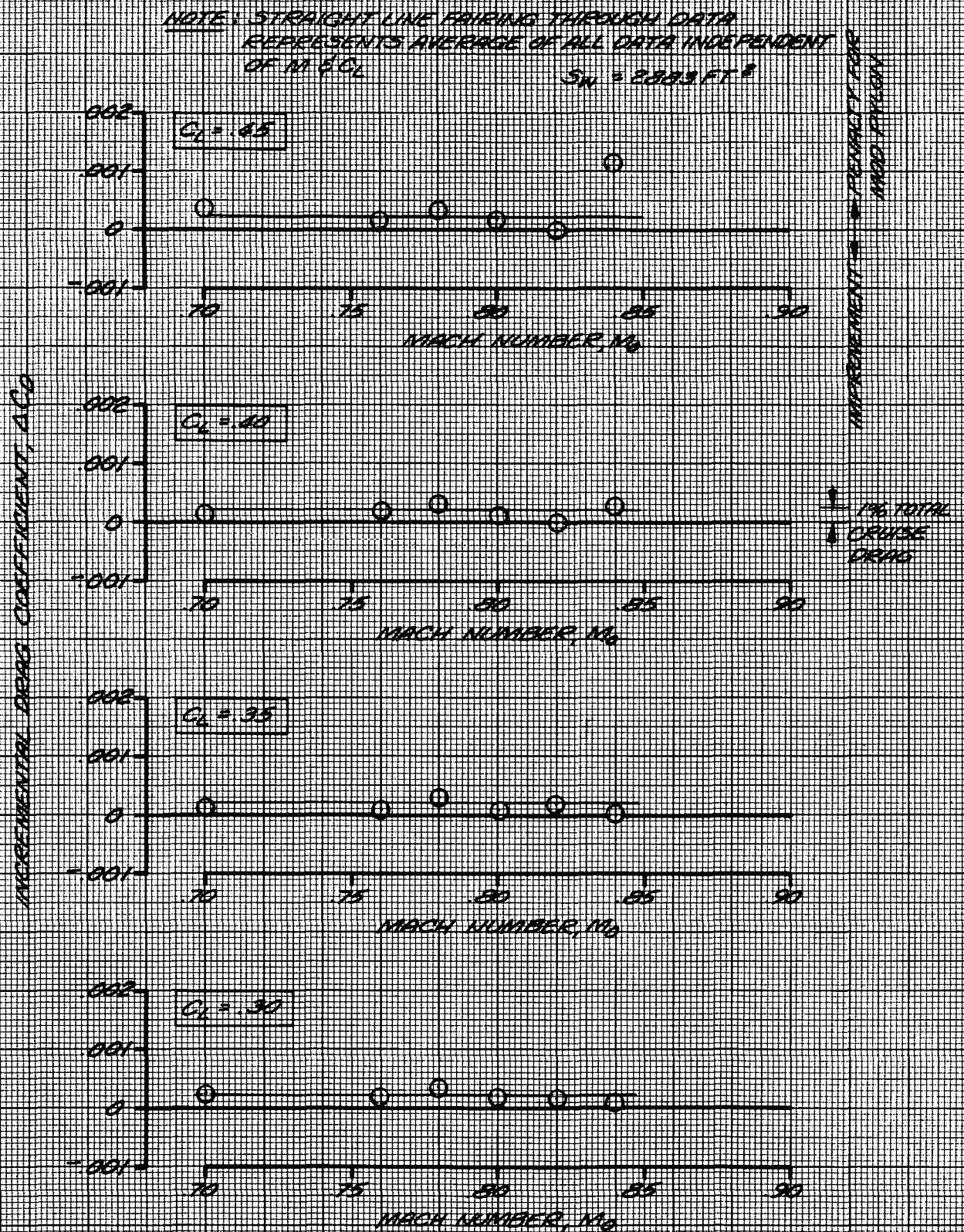


FIGURE 14: INCREMENTAL DRAG DUE TO ADDITION OF AFT-BLUMP TO BASIC REFIN PYLON



**DOUGLAS AIRCRAFT COMPANY**

3855 Lakewood Boulevard, Long Beach, California 90846 (213) 593-5511

**MCDONNELL DOUGLAS**

